Green Synthesis and Catalysis xxx (xxxx) xxx

Contents lists available at ScienceDirect

Green Synthesis and Catalysis

journal homepage: www.keaipublishing.com/en/journals/green-synthesis-and-catalysis

Research Article

Light-driven enzymatic conversion of mevastatin into pravastatin by coupling P450sca-2 with cyanobacterial photosynthetic system

Shanmin Zheng [a,b,1], Zhengquan Gao [a,1], Yuanyuan Jiang [b], Jiawei Guo [b], Fangyuan Cheng [b], Xuan Wang [b], Hao-Bing Yu [c], Bo Hu [c], Chunxiao Meng [a,*], Shengying Li [b,d,*], Xingwang Zhang [b,*]

[a] School of Pharmacy, Binzhou Medical University, Yantai 264003, China
[b] State Key Laboratory of Microbial Technology, Shandong University, Qingdao 266237, China
[c] Department of Marine Biomedicine and Polar Medicine, Naval Medical Center, Naval Medical University, Shanghai 200433, China
[d] Laboratory for Marine Biology and Biotechnology, Qingdao Marine Science and Technology Center, Qingdao 266237, China

ARTICLE INFO

Keywords:
Pravastatin
Cytochrome P450 enzymes
Cyanobacterial photosynthetic system
Light-driven P450 reactions
P450sca-2

ABSTRACT

Cytochrome P450 enzymes (P450s) are highly attractive green biocatalysts with application potential in fields of synthetic chemistry and synthetic biology. However, most P450 enzymatic reactions rely on expensive cofactor NAD(P)H and complex redox partner protein(s) to supply catalytically required electrons, which greatly limits their investigation and application. Here we develop a light-driven P450 system to transform mevastatin into pravastatin by coupling P450sca-2 from *Streptomyces carbophilus* with the photosynthetic machinery of the cyanobacterium *Synechococcus elongatus* PCC 7942 *via* their shared electron-transfer component ferredoxin. Using the extracted cyanobacterial thylakoid membrane as an electron generator and transporter, we show that the P450sca-2 catalyzed hydroxylation of mevastatin can be driven by visible light. We designed and tested three different light-driven P450 pathways by using water, artificial low-cost electron donors and *in situ* produced NADPH as electron sources and finally improved the product yields from 12.7 % to 70.1 %. Our results not only provide a 'green' approach for pravastatin production, but also demonstrate that the cyanobacterial thylakoid membrane can act as an efficient electron donor to drive P450 reactions *in vitro*, which can be applied in the construction of photosynthetic and CO_2-fixing P450 reaction systems in the future.

1. Introduction

Cytochrome P450 enzymes (P450s) are ubiquitously distributed in all kingdoms of life and hold the capability of catalyzing various types of oxidative reactions towards highly diverse substrates [1–3]. In particular, their ability to functionalize inert C–H bonds with high regio- and stereoselectivity, such as hydroxylation and epoxidation, has attracted great attention for their application potential in the field of green synthesis, especially for pharmaceutical synthesis [4–6].

Most P450 enzymes rely on redox partner protein(s) to deliver two electrons from an electron donor, such as NAD(P)H, to the heme-iron reactive center for O_2 activation and substrate oxidation [7,8]. For example, the bacterial type I P450s usually employ an iron-sulfur-containing ferredoxin (Fdx) and FAD-containing ferredoxin reductase (FdR) as their redox partners to shuttle electrons from NAD(P)H to P450s. However, in many cases, it is difficult/tedious to identify and obtain the native redox partners of a specific bacterial P450 due to the multiplicity and complexity of prokaryotic Fdxs and FdRs [9–11]. Meanwhile, exogenous redox partners often show low electron transfer efficiency when driving P450 reactions due to an uncoupled catalytic cycle [12]. These features make most of P450 catalytic systems complex, expensive, and inefficient, thus preventing these versatile biocatalysts from broader application.

Sunlight is an abundant and renewable source of energy to drive enzymatic reactions in nature [13]. For instance, the widespread Gram-negative cyanobacteria can capture sunlight and carry out photosynthesis *via* their photosynthetic systems [14,15]. In cyanobacterial cells, the light-driven reactions take place in the thylakoid membrane (TMe) to convert light energy into chemical energy in the forms of NADPH and ATP [16]. In this process, H_2O acts as the original electron donor and is oxidized by photosystem II (PSII) to generate O_2, H^+ and e^-. The produced electron is then delivered to photosystem I (PSI) *via* the

* Corresponding authors.
E-mail addresses: mengchunxiao@126.com (C. Meng), lishengying@sdu.edu.cn (S. Li), zhangxingwang@sdu.edu.cn (X. Zhang).
Peer review under the responsibility of Fudan University.
[1] These authors contributed equally to this work.

https://doi.org/10.1016/j.gresc.2024.07.001
Received 26 June 2024; Accepted 10 July 2024

plastoquinone (PQ) pool, cytochrome *b6f* (Cyt *b6f*), and plastocyanin (PC, or cytochrome C6 (Cyt C6) in some cyanobacteria) cascade. Subsequently, the single electron carrier Fdx, which could also act as the redox partner of type I P450s [9], transfers the electron from PSI to FdR to reduce $NADP^+$ into NADPH, which further drives ATP production (Fig. 1).

Interestingly, the photosynthetic pathway and P450 catalytic system both employ Fdx and FdR to shuttle electrons, though in opposite directions. Thus, in principle, the shared Fdx could be harnessed to transfer photosynthesis-generated electrons from the electron transport chain to an Fdx-specific P450 to achieve 'light-driven P450 reaction', which would be able to use light as energy source and H_2O as electron donor (Fig. 1). Previously, several studies attempted to drive P450 reactions with light by expressing an exogenous P450 onto the cyanobacterial TMe *in vivo* or by combining the extracted PSI with P450s *in vitro* with 2,6-dichlorophenolindopheno (DCPIP) and sodium ascorbate (Asc) as artificial electron sources [17–22]. However, owing to the complex reaction environment *in vivo*, it is still questionable whether the introduced P450 enzyme specifically used the photosystem supplied electrons or the electrons transferred from the intracellular redox partner proteins (or both). Furthermore, it is also short of evidence that if the entire TMe could support P450 reactions by using water as an electron source *in vitro*.

In this study, we utilize the full function of extracted cyanobacterial TMe from *Synechococcus elongatus* PCC 7942 to support the mevastatin-to-pravastatin reaction catalyzed by P450sca-2 from *Streptomyces carbophilu in vitro*. Our results clearly show that cyanobacterial TMe can well support the regio- and stereoselective hydroxylation reaction in a light-dependent manner with a maximum yield of 70.1 %. This not only provides a 'green' approach for pravastatin production, but also demonstrates the full photosynthetic enzymatic machinery can serve as an *in vitro* electron supplier for exogenous P450s with possible utility in both academic research and practical application.

2. Results and discussion

2.1. Design of the in vitro light-driven P450 reaction system

Pravastatin is a first-line lipoprotein-lowering drug for managing and treating primary hypercholesterolemia, hyperlipidemia, and mixed dyslipidemia [23,24]. P450sca-2 (*i.e.*, CYP105A3), a type I P450 screened from *S. carbophilus*, is able to catalyze the selective 6β-hydroxylation of mevastatin to produce pravastatin, thus holding great potential in industrial application for pravastatin production [25]. In this study, we selected P450sca-2 as a testing P450 enzyme to couple with cyanobacterial TMe in order to explore the feasibility of light-driven and TMe-mediated P450 reaction *in vitro*. The model cyanobacterial strain *S. elongatus* PCC 7942 was selected as a source for TMe preparation.

The TMe-associated entire electron transport chain for photosynthesis includes PSI, PSII, PQ, Cyt *b6f*, PC/Cyt C6, and Fdx (Fig. 1). According to the current understanding [26,27], the membrane-bound PSI, PSII, and Cyt *b6f*, as well as the PQ pool, should be tightly anchored inside TMe, while PC/Cyt C6 and Fdx that cooperate with the electron transport chain in a dynamic interaction manner (Fig. 1) might be lost during the TMe preparation process. Thus, we supplied the *S. elongatus* PCC 7942 derived Cyt C6, Fdx and FdR *in trans* in the TMe-P450 assay in order to reconstitute the entire photosynthetic pathway *in vitro*.

2.2. Light-driven P450sca-2 reaction using H_2O as an electron donor

To achieve light-driven conversion from mevastatin to pravastatin, we started to solely use TMe to supply electrons for P450sca-2. In this pathway, PSII in TMe first photolyzes H_2O to generate electrons, which are then sequentially transferred to Fdx and shuttled to P450sca-2 *via* protein-protein interactions (Fig. 1, path i). Experimentally, 100 μmol/L mevastatin was incubated with 1 μmol/L P450sca-2, 10 μmol/L Fdx, 10 μmol/L Cyt C6 and 20 μg chlorophyll equivalent of TMe. In addition, 50 mg/mL catalase was added into the reaction mixture to avoid the

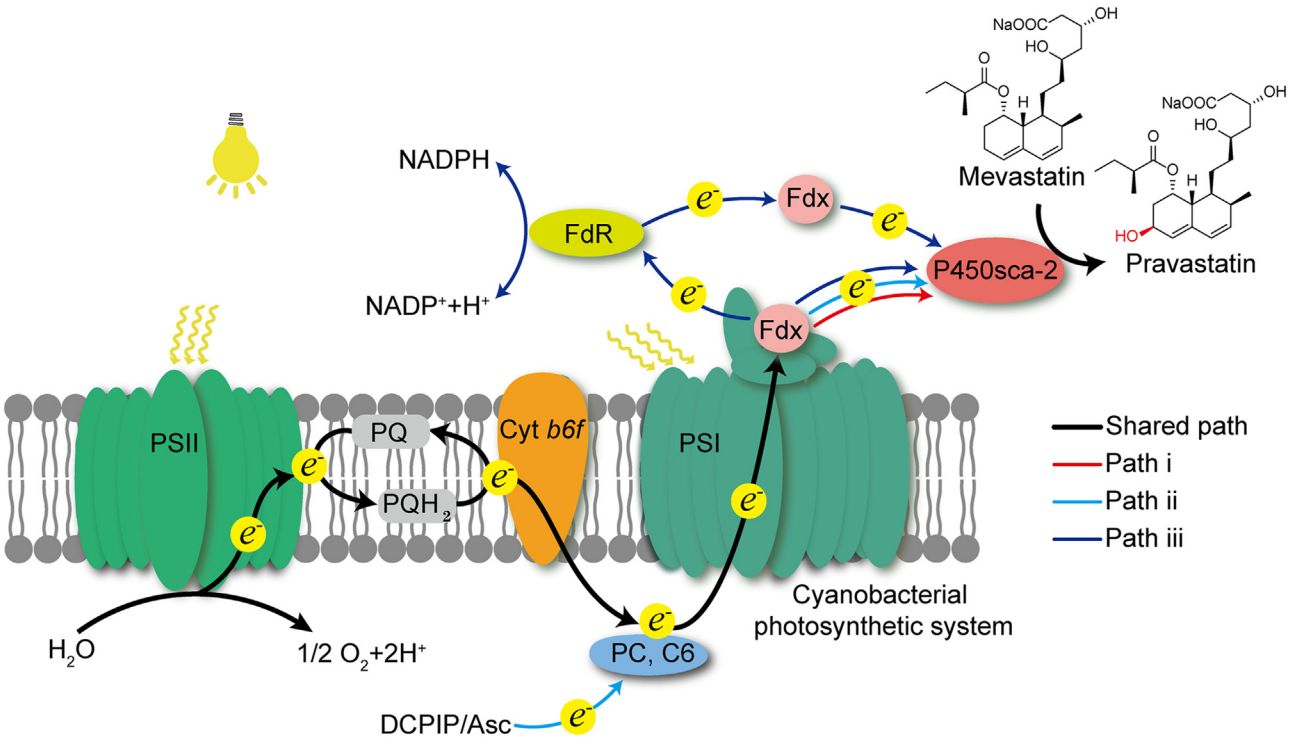

Fig. 1. The representative cyanobacterial photosynthetic system and the designed electron-transfer pathways for the light-driven P450sca-2 reactions (adopted from Ref. [8]). PSII: photosystem II; PQ: plastoquinone; Cyt *b6f*: cytochrome *b6f*; PC: plastocyanin; C6: cytochrome C6; DCPIP: 2,6-dichlorophenolindopheno; Asc: sodium ascorbate; PSI: photosystem I; Fdx: ferredoxin; FdR: ferredoxin reductase.

influence of reactive oxygen species (ROS) on P450. The reactions were incubated under illumination conditions using a fluorescent lamp at 25 °C for 12 h. The negative controls were performed in parallel using boiling-inactivated TMe or incubated in the dark. For the positive control, we used *S. elongatus* PCC 7942 derived Fdx1499 and FdR0978 as surrogate redox partners to drive the P450sca-2 reaction using NADPH as an electron source.

As expected, ultra-performance liquid chromatography (UPLC) analysis showed the production of pravastatin in the light-driven reaction by comparing the retention time and high-resolution electrospray ionization-mass spectrometry (HRESI-MS) data with the pravastatin authentic standard (Fig. 2A). Meanwhile, no product was detected from the control reactions that were either incubated in dark or utilized the boiling-inactivated TMe. These results clearly demonstrated that TMe could act as an electron donor to drive the P450 reaction in a light-dependent manner, despite that the catalytic efficiency was much lower than the P450sca-2 reaction supported by the NADPH-FdR-Fdx system, which can completely convert mevastatin (Fig. 2A).

To further improve the catalytic efficiency, we tested the optimal concentration of Fdx and Cyt C6. Specifically, we conducted the light-driven P450sca-2 reactions under varying concentrations of Fdx and Cyt C6, individually ranging from 0 to 50 μmol/L for Fdx and from 0 to 20 μmol/L for Cyt C6. UPLC analysis of the product yield revealed 30 μmol/L of Fdx and 1 μmol/L of Cyt C6 to be the optimal concentrations for the two proteins (Fig. 2B and C). Thereafter, we performed a time-course experiment using the optimized enzyme concentrations. The results showed that the product yield stabilized at 8 h and reached the maximum (12.7 ± 0.2 %) at 12 h (Fig. 2D). These results together confirmed the feasibility of using TMe as an electron donor to support P450 reactions and the catalytic efficiency of the light-driven system can be improved by cofactor concentration adjustment.

2.3. Improving product yield by artificial electron supplement

It was reported that the mixture of DCPIP and Asc could act as a redox mediator, as well as an electron supplier, for PSI [20,21,28]. Therefore, to further improve the catalytic efficiency of the light-driven P450sca-2 reaction, we added the DCPIP/Asc solution into the P450sca-2/mevastatin reaction. In this alternative system, in addition to the PSII generated electrons, PSI (under light conditions) could also shuttle exogenous electrons from DCPIP/Asc through PC/Cyt C6 (Fig. 1, path ii). As anticipated, the reaction involving DCPIP/Asc under illuminated conditions led to higher production of pravastatin when compared to that of path i. By contrast, the control reactions, which were incubated in the absence of either light or active TMe, did not result in any product formation (Fig. 3A).

Next, we attempted to optimize the concentrations of Fdx and Cyt C6 for this system. The concentration-gradient experiments indicated that the optimal concentration of Fdx should be 30 μmol/L (Fig. 3B), which is consistent with that of path i. However, the experiments involving a gradient of Cyt C6 concentration revealed that the inclusion of this protein diminished the production of pravastatin, even at low concentrations (Fig. 3C). It was observed that the yields of the product significantly decreased when the concentration of Cyt C6 escalated from 0 to 10 μmol/L, and then stabilized at a yield comparable to the reaction without DCPIP/Asc (Fig. 3C). These findings suggest that the addition of Cyt C6 would deplete DCPIP/Asc in a protein concentration-dependent manner, and also imply that the naturally bound PC/Cyt C6 in TMe should be sufficient to facilitate electron transfer from DCPIP/Asc to PSI.

Finally, the time-course experiments with the optimized protein concentrations revealed that the yields of pravastatin peaked at 19.2 ± 0.4 % after a reaction duration of 4 h, and subsequently remained stable (Fig. 3D). These findings underscored that the catalytic efficiency of the light-driven P450 reaction could be enhanced through the supplementation of a low-cost artificial electron donor [20,21].

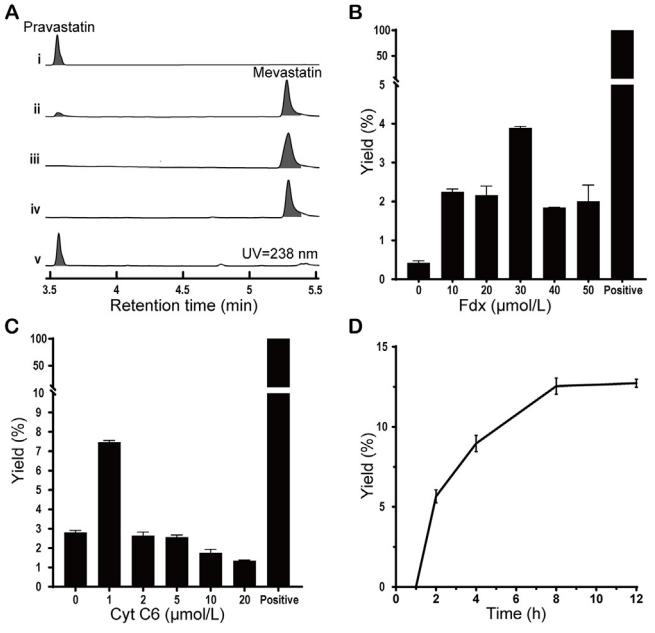

Fig. 2. Product analysis and reaction optimization of path i. (A) UPLC analysis of the path i reactions and related control reactions. **i**: the standard of pravastatin; **ii**: the path i reaction incubated under light condition, **iii**: the path i reaction incubated in darkness; **iv**: control of **ii** using boiling-inactivated TMe, **v**: P450sca-2 reaction supported by Fdx-FdR-NADPH. (B) Fdx concentration optimization results. (C) Cyt C6 concentration optimization results. (D) Time-course experiment results of path i reactions using optimal concentrations of Fdx and Cyt C6. Error bars represent the standard deviation calculated from two independent experiments, the same below.

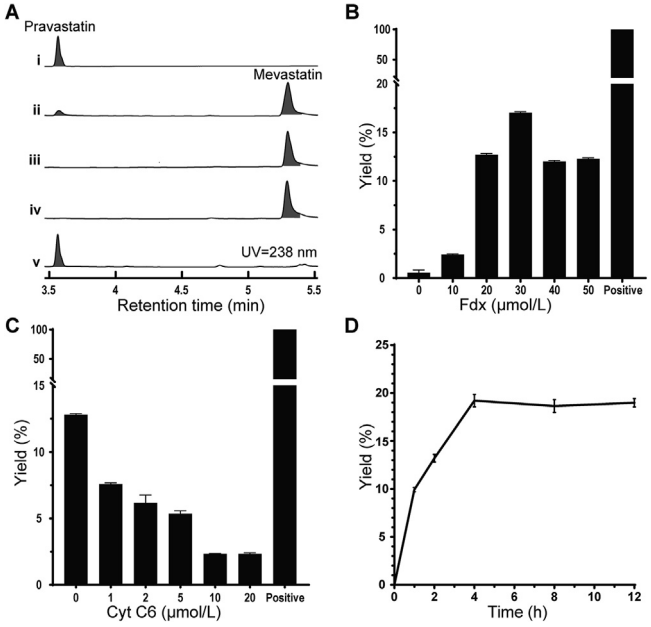

Fig. 3. Product analysis and reaction optimization of path ii. (A) UPLC analysis of the path ii reactions and related control reactions. **i**: the standard of pravastatin; **ii**: the path ii reaction incubated under light condition, **iii**: the path ii reaction incubated in darkness; **iv**: control of ii using boiling-inactivated TMe, **v**: P450sca-2 reaction supported by Fdx-FdR-NADPH. (B) Fdx concentration optimization results. (C) Cyt C6 concentration optimization results. (D) Time-course experiment results of path ii reactions using optimal concentrations of Fdx and Cyt C6.

2.4. Enhancing catalytic efficiency through in situ NADPH production

Despite the enhancement of the catalytic efficiency of the TMe-supported P450sca-2 reaction through reaction optimization and artificial electron supplementation, the substrate conversion ratio remained significantly lower than that of the redox partner-supported reaction which can completely convert mevastatin into pravastatin (Figs. 2A and 3A). We ascribed the diminished catalytic efficiency to the suboptimal coupling efficiency between the PSI anchored Fdx and P450sca-2 through protein-protein interactions [29]. To address this issue, we proposed the construction of a complete photosynthetic pathway for NADPH production, which would act as an electron pool to provide additional electrons to augment the catalytic activity of P450sca-2 (Fig. 1, path iii). In this pathway, a fraction of electrons delivered by Fdx would be directed to P450sca-2, while the remaining would be transferred to FdR for NADPH production. The NADPH produced *in situ* could then serve as an auxiliary electron donor for P450sca-2, facilitated by the electron transfer bridge comprising of FdR and Fdx (Fig. 1, path iii).

To test this hypothesis, we first measured NADPH production with TMe by adding FdR and $NADP^+$ into the photosynthetic reaction. The results showed that the photosynthetic system indeed produced enough NADPH to serve as electron sources for P450sca-2 (Fig. 4A). However, the control reactions which were incubated in the dark also produced minor NADPH (Fig. 4A). It was previously reported that the oxidative pentose phosphate pathway (OPPP) in cyanobacteria can degrade glycogen to generate NADPH in dark stage [30,31]. Thus, it was supposed that the extracted crude TMe component should contain enzymes and cofactors of OPPP, which can produce NADPH under dark conditions. Then, we further added 1 μmol/L FdR and 3 mmol/L $NADP^+$ into the path i reaction (without any artificial electron sources). As expected, the yield of pravastatin exhibited an increase compared to that of paths i and ii (Fig. 4B). In addition, a minor quantity of pravastatin was also detected in the control reaction incubated in dark conditions, which could be fairly attributed to the product of OPPP produced NADPH supported P450sac-2 reaction.

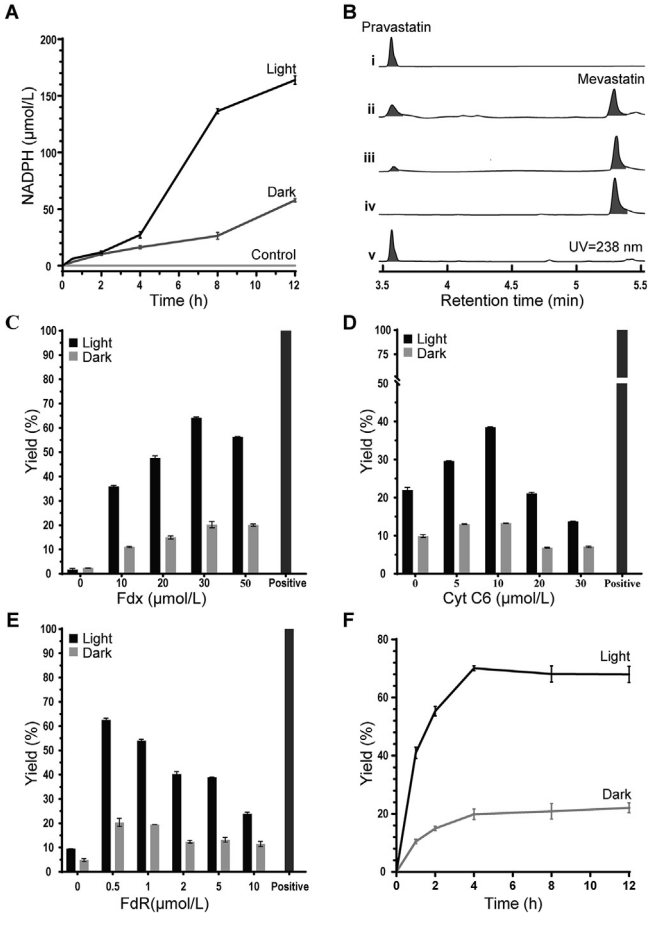

Fig. 4. Product analysis and reaction optimization of path iii. (A) NADPH production analysis. (B) UPLC analysis of the path iii reactions and related control reactions. **i**: the standard of pravastatin; **ii**: the path iii reactions incubated under light condition, **iii**: the path iii reactions incubated in darkness; **iv**: control of **ii** using boiling-inactivated enzymes, **v**: P450sca-2 reaction supported by Fdx-FdR-NADPH. (C–E) Protein concentration optimization results of Fdx (C), Cyt C6 (D), and FdR (E). (F) Time-course experiment results of path iii reactions using optimal concentrations of Fdx and Cyt C6 and FdR. The markers 'Light' and 'Dark' indicate the reactions were incubated under light and dark conditions, respectively.

Next, we sought to optimize the protein concentrations of Fdx, Cyt C6, and FdR, individually. The results indicated that the optimal concentrations for Fdx, Cyt C6, and FdR under the light conditions were 30, 10, and 0.5 μmol/L, respectively (Fig. 4C, D, E). Subsequently, we employed the optimized protein concentrations to facilitate the reactions in time-course experiments. The results indicated that the production of pravastatin plateaued after a reaction duration of 4 h, with the maximum yield reaching 70.1 ± 0.6 % (Fig. 4F), demonstrating that the catalytic efficiency can be significantly enhanced by incorporating the NADPH production and utilization cycle (Fig. 1, path iii). This improvement can be attributed to at least two factors: a) NADPH is a natural product of the TMe photosynthetic system, which may potentially accelerate the overall reactivity of the photosynthetic system, and b) NADPH also serves as the native electron donor of P450sca-2, thus providing a more favorable electron supply chain for P450sca-2 *via* FdR-Fdx.

Taken together, our findings unequivocally illustrate that the cyanobacterial TMe can effectively couple with an exogenous P450 enzyme, through their shared electron-transfer protein Fdx, to realize a proof-of-concept light-driven P450 reaction *in vitro*.

3. Conclusion

Herein, we achieved a light-driven P450 reaction by integrating cyanobacterial TMe with P450sca-2 *in vitro*, thereby transforming mevastatin into pravastatin. We strategically devised three pathways to improve the efficiency of the light-driven P450 reactions, giving a substantial enhancement in product yield from 12.7 % to 70.1 %. The implementation of light-driven P450 reactions circumvents the necessity for the costly cofactor NADPH and intricate specific redox partners, conferring benefits in terms of cost reduction and CO_2 emission mitigation. We anticipate that the employment of TMe as a general electron donor for P450 reactions will pave a new avenue for P450 research and application in the future.

4. Experimental

4.1. Protein activity detection

The activity and concentrations of purified P450sca-2 [32], Fdx and FdR [33] (Fig. S1) were determined according to the previously established methods. The functional concentration of P450sca-2 was measured from the CO-bound reduced difference spectrum (Supporting Information Fig. S2) using the extinction coefficient ($\epsilon_{450\text{-}490}$) of 91,000 L/(mol·cm) according to the previously established procedure [34]. The concentration of cytochrome P450 was calculated using the following formula:

$$C_{P450sca\text{-}2}\ (\mu mol/L) = (\Delta A450 - \Delta A490) / 91000 \times 10^6 \times \text{dilution factor}.$$

And Fdx and FdR have an absorbance coefficient of 9700 L/(mol·cm) at 420 nm and 10400 L/(mol·cm) at 456 nm, respectively. The protein concentrations were calculated using the spectrophotometric method, and the formulas used were as follows:

C_{Fdx} (μmol/L) = A420/9700 × 10^6 × dilution factor;

C_{FdR} (μmol/L) = A456 / 10400 × 10^6 × dilution factor.

After *Cyt C6* was cloned (Fig. S3) and heterologously expressed in *E. coli*, the activity and concentration of Cyt C6 were determined by measuring the specific absorbance spectrum between 350 and 600 nm (Fig. S4) [35]. The molar absorption coefficient of Cyt C6 at 553 nm was 26200 L/(mol·cm). The protein concentration was determined using the spectrophotometric method by following the formula:

$C_{Cyt\ C6}$ (μmol/L) = A553/26200 × 10^6 × dilution factor.

4.2. Preparation of thylakoid membranes

Extraction of TMe was carried out by following the previously reported procedure [36]. Briefly, the collected *S. elongatus* PCC 7942 cells from 1 L culture were washed twice with BG11 medium, and then suspended with 15 mL buffer A (25 mmol/L MES-NaOH, pH 6.5, 10 mmol/L $CaCl_2$, 10 mmol/L $MgCl_2$, 25 % glycerol). Glass beads (221–300 μm) were added in an equal volume, and the mixture was subjected to vortex shaking at maximum speed for 20 s, followed by a 1 min cooling period. The cycle was repeated for 5 times to crush the cell walls. The suspension was centrifuged at 4 °C, 3,000 *g* for 2 min to collect the supernatant. Then, 20 mL of buffer A was further added to the remaining precipitation and shaken for twice, and again centrifuged to collect the supernatant. The two supernatants were combined and centrifuged to remove the intact cells and glass beads. After that, the supernatant was centrifuged at 4 °C, 180,000 *g* for 45 min to collect the pellet. The TMe-containing pellet was finally suspended in buffer A for concentration determination and enzymatic assays.

The chlorophyll (Chl) content in the TMe suspension was measured as follows: 13.5 μL aliquot of the suspension was mixed with 1.5 μL of 10 % *n*-dodecyl-*β*-D-maltoside (DM), then centrifuged at 16,000 *g* for 5 min, and 10 μL of the supernatant was transferred to 990 μL of methanol. After vortexing, the mixture was centrifuged at 16,000 *g* for 5 min, and the supernatant was collected. The absorbance spectrum was recorded at 350–750 nm (Fig. S5), and then the Chl content was calculated using the following formula [37]:

C_{TMe} (μg Chl/mL) = (12.25 × A663–2.79 × A645) × dilution factor.

4.3. Enzymatic assays and product analysis

Each reaction was performed in a 500 μL quartz tube, using a Rishang Lighting YZ08-75 fluorescent tube with two light sources (8 W). The reaction buffer contained 1 mmol/L EDTA, 50 mmol/L NaH_2PO_4, 0.5 mmol/L dithiothreitol (DTT), and 10 % glycerol (pH 7.4). All enzymatic assays were performed at 25 °C in a 100 μL reaction system, and the boiling-inactivated enzymes were used for negative control reactions. Each reaction was divided into two parts and respectively incubated under light and dark conditions for 12 h. The time-course experiments were carried out with a timeline of 0, 1, 2, 4, 8 and 12 h.

Afterwards, the reaction was terminated by thoroughly mixing with 200 μL methanol, and the mixture was high-speed centrifuged (12,000 *g*, 10 min, 16 °C) to remove the metamorphic proteins. The supernatants were analyzed with High Performance Liquid Chromatography (HPLC) or UPLC. The substrate and product were quantified by fitting to the standard curves of mevastatin and pravastatin, respectively. The product yield was calculated by "yield (%) = (mol of the product yielded/mol of the product expected) × 100 %".

4.4. NADPH production assays

In the experiments to test NADPH production with the photosynthetic system, the reactions were performed at 25 °C in a 100 μL reaction system under light conditions, and control reactions without TMe or incubated in the dark were performed in parallel. The reaction system contained 10 μmol/L Fdx, 10 μmol/L Cyt C6, 1 μmol/L FdR, 20 μg chlorophyll equivalent of TMe and 3 mmol/L $NADP^+$. Reactions were quenched at 0, 0.5, 2, 4, 8 and 12 h by adding 200 μL methanol, and the mixtures were then high-speed centrifuged (12,000 *g*, 10 min, 16 °C) to remove the metamorphic proteins. NADPH production was tested and calculated using the spectrophotometric method according to the molar absorption of NADPH at 340 nm of 6300 L/(mol·cm), NADPH content was calculated using the following formula [38]:

C_{NADPH} (μmol/L) = A340 / 6300 × 10^6.

CRediT authorship contribution statement

Shanmin Zheng: Data curation, Formal analysis, Investigation, Writing – original draft. **Zhengquan Gao:** Conceptualization, Resources, Writing – original draft, Funding acquisition. **Yuanyuan Jiang:** Formal analysis, Supervision. **Jiawei Guo:** Formal analysis. **Fangyuan Cheng:** Formal analysis. **Xuan Wang:** Formal analysis. **Hao-Bing Yu:** Formal analysis. **Bo Hu:** Formal analysis. **Chunxiao Meng:** Conceptualization, Supervision, Writing – review & editing, Funding acquisition. **Shengying Li:** Conceptualization, Supervision, Writing – review & editing, Funding acquisition. **Xingwang Zhang:** Conceptualization, Formal analysis, Funding acquisition, Writing – review & editing.

Declaration of competing interest

The authors declare that they have no known competing financial interests or personal relationships that could have appeared to influence the work reported in this paper.

Acknowledgements

This work was supported by the National Key R&D Program of China [No. 2023YFA0915500], the National Natural Science Foundation of China [Nos. 32025001, 42176124], the Shandong Provincial Natural Science Foundation [Nos. ZR2019ZD20, ZR2019ZD17, ZR2021MC051 and ZR2023ZD50], State Key Laboratory of Microbial Technology Open Projects Fund [No. M2023-01], Fujian Province Universities and Colleges Technology and Engineering Center for Marine Biomedical Resource, Xiamen Medical College [No. xmmc-mnpr-2022001] and the Yantai Economic-Technological Development Area Innovation Pilot Project [No. 2021RC007]. The authors thank Jingyao Qu, Guannan Lin, Jing Zhu and Zhifeng Li from the State Key Laboratory of Microbial Technology at Shandong University for their guidance and help in HPLC and MS analysis.

Appendix A. Supplementary data

Supplementary data to this article can be found online at https://doi.org/10.1016/j.gresc.2024.07.001.

References

[1] P. Durairaj, S. Li, Eng. Microbiol. 2 (2022) 100011.
[2] X. Zhang, S. Li, Nat. Prod. Rep. 34 (2017) 1061–1089.
[3] X. Zhang, J. Guo, F. Cheng, S. Li, Nat. Prod. Rep. 38 (2021) 1047–1228.
[4] R.W. Estabrook, K.M. Faulkner, M.S. Shet, C.W. Fisher, Methods Enzymol. 272 (1996) 44–51.
[5] P.R.O.D. Montellano, Fourth Ed Book Cytochrome P450-Structure, Mechanism, and Biochemistry, Springer, Switzerland, 2015.
[6] R.J. Li, Z. Zhang, C.G. Acevedo Rocha, J. Zhao, A. Li, Green, Synth. Catal. 1 (2020) 52–59.
[7] J.D. Rudolf, C.Y. Chang, M. Ma, B. Shen, Nat. Prod. Rep. 34 (2017) 1141–1172.
[8] S. Zheng, J. Guo, F. Cheng, Z. Gao, L. Du, C. Meng, S. Li, X. Zhang, Acta Pharm. Sin. B 12 (2022) 2832–2844.
[9] S. Li, L. Du, R. Bernhardt, Trends Microbiol. 28 (2020) 445–454.

[10] S. Li, L.M. Podust, D.H. Sherman, J. Am. Chem. Soc. 129 (2007) 12940–12941.
[11] X. Liu, F. Li, T. Sun, J. Guo, X. Zhang, X. Zheng, L. Du, W. Zhang, L. Ma, S. Li, Commun. Biol. 5 (2022).
[12] W. Zhang, L. Du, F. Li, X. Zhang, Z. Qu, L. Han, Z. Li, J. Sun, F. Qi, Q. Yao, Y. Sun, C. Geng, S. Li, ACS Catal. 8 (2018) 9992–10003.
[13] A.K. Ringsmuth, M.J. Landsberg, B. Hankamer, Renew. Sustain. Energy Rev. 62 (2016) 134–163.
[14] L.M. Lassen, A.Z. Nielsen, B. Ziersen, T. Gnanasekaran, B.L. Moller, P.E. Jensen, ACS Synth. Biol. 3 (2014) 1–12.
[15] R.B. Dixit, M.R. Suseela, Anton. Leeuw. Int. J. G. 103 (2013) 947–961.
[16] N. Nelson, W. Junge, Annu. Rev. Biochem. 84 (2015) 659–683.
[17] L.M. Lassen, A.Z. Nielsen, C.E. Olsen, W. Bialek, K. Jensen, B.L. Moller, P.E. Jensen, PLoS One 9 (2014) 1–10.
[18] A. Wlodarczyk, T. Gnanasekaran, A.Z. Nielsen, N.N. Zulu, S.B. Mellor, M. Luckner, J.F.B. Thofner, C.E. Olsen, M.S. Mottawie, M. Burow, M. Pribil, I. Feussner, B.L. Moller, P.E. Jensen, Metab. Eng. 33 (2016) 1–11.
[19] D. Kannchen, J. Zabret, R. Oworah-Nkruma, N. Dyczmons-Nowaczyk, K. Wiegand, P. Lobbert, A. Frank, M.M. Nowaczyk, S. Rexroth, M. Rogner, BBA-bioenergetics, vol. 1861, 2020, pp. 148208–148218.
[20] K. Jensen, P.E. Jensen, B.L. Moller, ACS Chem. Biol. 6 (2011) 533–539.
[21] K. Jensen, J.B. Johnston, P.R. de Montellano, B.L. Moller, Biotechnol. Lett. 34 (2012) 239–245.
[22] V. Jurkaš, C.K. Winkler, S. Poschenrieder, P. Oliveira, C.C. Pacheco, E.A. Ferreira, F. Weissensteiner, P. De Santis, S. Kara, R. Kourist, P. Tamagnini, W. Kroutil, Eng. Microbiol. 2 (2022) 100008.
[23] N. Serizawa, S. Serizawa, K. Nakagawa, K. Furuya, T. Okazaki, A. Terahara, J. Antibiot. 36 (1983) 887–891.
[24] N. Serizawa, K. Nakagawa, K. Hamano, Y. Tsujita, A. Terahara, H. Kuwano, J. Antibiot. 36 (1983) 604–607.
[25] T. Matsuoka, S. Miyakoshi, K. Tanzawa, K. Nakahara, M. Hosobuchi, N. Serizawa, Eur. J. Biochem. 184 (1989) 707–713.
[26] N. Nelson, C.F. Yocum, Annu. Rev. Plant Biol. 57 (2006) 521–565.
[27] N. Nelson, A. Ben-Shem, Nat. Rev. Mol. Cell Biol. 5 (2004) 971–982.
[28] A. Petrova, M. Mamedov, B. Ivanov, A. Semenov, M. Kozuleva, Photosynth. Res. 137 (2018) 421–429.
[29] N. Fischer, M. Hippler, P. Sétif, J.P. Jacquot, J.D. Rochaix, EMBO J. 17 (1998) 849–858.
[30] D.G. Welkie, B.E. Rubin, S. Diamond, R.D. Hood, D.F. Savage, S.S. Golden, Trends Microbiol. 27 (2019) 231–242.
[31] J. Hatano, S. Kusama, K. Tanaka, A. Kohara, C. Miyake, S. Nakanishi, G. Shimakawa, Photosynth. Res. 153 (2022) 113–120.
[32] T. Omura, R. Sato, J. Biol. Chem. 239 (1964) 2379–2385.
[33] C.J. Batie, H. Kamin, J. Biol. Chem. 256 (1981) 7756–7763.
[34] Y. Jiang, Z. Li, S. Zheng, H. Xu, Y.J. Zhou, Z. Gao, C. Meng, S. Li, Biotechnol. Biofuels 13 (2020) 52.
[35] F.P. Molina-Heredia, M. Hervas, J.A. Navarro, M.A. De la Rosa, Biochem. Biophys. Res. Commun. 243 (1998) 302–306.
[36] L.S. Zhao, T. Huokko, S. Wilson, D.M. Simpson, Q. Wang, A.V. Ruban, C.W. Mullineaux, Y.Z. Zhang, L.N. Liu, Nat. Plants 6 (2020) 869–882.
[37] K. Baba, S. Itoh, G. Hastings, S. Hoshina, Photosynth. Res. 47 (1996) 121–130.
[38] F. Li, X. Wei, L. Zhang, C. Liu, C. You, Z. Zhu, Angew. Chem. Int. Ed. 61 (2022) e202111054.